

Letters

A Modular Multilevel Converter with a Zigzag Transformer for Bipolar MVDC Distribution Systems

Shenghui Cui , Joon-Hee Lee, Jingxin Hu , Rik W. De Doncker, and Seung-Ki Sul 

Abstract—This letter presents a modular multilevel converter (MMC) for bipolar medium-voltage direct-current (MVDC) distribution systems. By employing a zigzag transformer as a grid interface transformer with a dedicated operation method, the operation of two dc poles of an MMC can be fully decoupled. Consequently, the MMC can provide full bipolar-operation capability. No additional component is required, and no penalty of increased power rating is imposed on the grid interface transformer. The scheme based on the proposed topology is competitive and cost-effective for emerging MVDC distribution systems. Feasibility of the proposed scheme is verified by both simulations and down-scale experiments.

Index Terms—Bipolar dc grid, dc distribution, modular multilevel converter (MMC), zigzag transformer.

I. INTRODUCTION

THE dc distribution is a key-enabling technology for future decentralized power grids, which will integrate a great amount of renewable energy and energy storage [1]. Compared to the ac distribution, the dc distribution has higher efficiency, higher reliability, and higher flexibility.

There are two types of dc distribution systems: the monopole configuration and the bipolar configuration, as shown in Fig. 1(a) and (b), respectively. Compared to the monopole configuration, a bipolar distribution system has significant advantages of, e.g., providing different voltage levels similar to a three-phase ac system and increased reliability due to the independent operation of two poles [2].

In order to establish a bipolar dc distribution system, two ac-dc converters e.g., two-level converters (TLC) with galvanically isolated ac sides are required, as shown in Fig. 1(b). It increases the system complexity, and the secondary side of the transformer is subjected to a dc offset voltage with respect to the ground. To address this issue, a general approach is employing an auxiliary

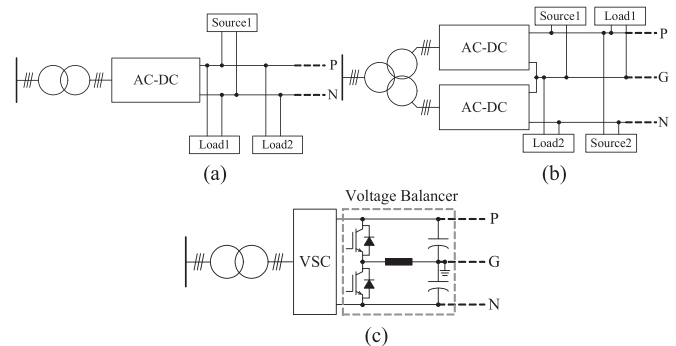


Fig. 1. Conceptual configurations of dc distribution systems. (a) Monopole dc system. (b) Bipolar dc system with two ac-dc converters. (c) Bipolar dc system with a single ac-dc converter and a voltage balancer.

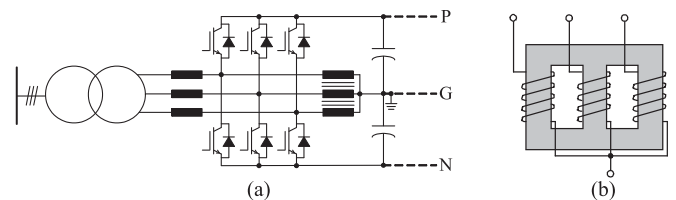


Fig. 2. TLC with a grounding inductor for bipolar dc distribution systems. (a) Circuit diagram. (b) Grounding inductor structure.

voltage balancer to maintain the dc pole voltage balanced in case of a power unbalance [3]–[6], as shown in Fig. 1(c). The main drawback of this approach is that it requires an extra power-electronic converter as the voltage balancer.

A three-level converter with two split dc-link capacitors, e.g., a neutral-point clamped converter or a T-type converter can establish a bipolar dc-link voltage by controlling the dc-link neutral-point current via manipulating the zero-sequence voltage reference [12]. However, the unbalanced-operation capability of two dc-link poles is very limited due to the dependency of the maximum available neutral-point current on the ac-side current magnitude and phase [13], and it is not suitable for establishing a bipolar dc distribution system. Thus, it is concluded in [3] that an auxiliary balancing leg has to be added in order to enable a full bipolar operation capability.

A novel approach of integrating a voltage balancer into a TLC was proposed in [7], as shown in Fig. 2(a). A three-phase grounding inductor was connected on the ac terminal of the

Manuscript received May 15, 2018; revised June 19, 2018; accepted July 7, 2018. Date of publication July 10, 2018; date of current version December 7, 2018. (Corresponding author: Shenghui Cui.)

S. Cui, J. Hu, and R. W. De Doncker are with E.ON Energy Research Center, RWTH Aachen University, Aachen 52062, Germany (e-mail:

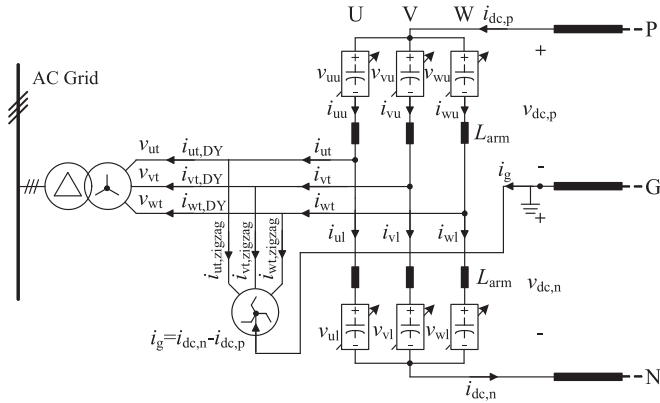


Fig. 3. MMC with an auxiliary zigzag grounding transformer for bipolar operation capability.

TLC to provide a current path from the ac side to the dc-side neutral so that the positive and negative poles on the dc side can be controlled independently. A three-limb core inductor shown in Fig. 2(b) was employed as a grounding inductor due to the following reasons: 1) a three-limb core inductor presents large positive- and negative-sequence impedance, which results in low reactive-power consumption and 2) a three-limb core inductor presents small zero-sequence impedance, which leads to a fast response of the zero-sequence current and enables a fast dynamic control of two dc poles.

However, the aforementioned concept proposed in [7] has several crucial drawbacks. The grounding inductor is subjected to the transformer secondary-side voltage and two-thirds of the rated dc-link current would flow through each winding of the inductor. Thus, the power rating of the grounding inductor is 70%–80% of that of the transformer. Moreover, the inductance has to be very large in order to decrease the reactive-power consumption and it would result in high conductive losses. In case of the power unbalance at dc poles, a zero-sequence dc current flows through the grounding inductor and induces significant zero-sequence MMF. Due to the lack of the zero-sequence magnetic return path in the three-limb core inductor, the magnetic flux returns outside the core and might result in interference to surrounding electronic components [8]. In addition, such a concept is applicable to two-/three-level VSCs and is not suitable for medium-voltage direct-current (MVDC) distribution where the dc voltage is in the range of dozens of kV.

In [9], an auxiliary zigzag transformer is proposed as a grounding device for symmetric monopole modular multilevel converter (MMC)-HVDC systems in order to provide a virtual neutral point for grounding purpose and keep balance between the positive- and negative-pole-to-ground voltages of the HVDC cables. Besides the aforementioned functionalities proposed in [9], the auxiliary zigzag grounding transformer can also be used to establish a bipolar dc-link for a voltage-source converter, e.g., a TLC or an MMC, as shown in Fig. 3. Such a configuration can enable a full bipolar operation capability, as presented in Section IV of this letter. Unfortunately, no operation method or control scheme on bipolar operation is discussed in [9]. One crucial drawback of the configuration shown in Fig. 3 is that a significant dc current flows through the zigzag transformer winding in case of unbalanced dc-link pole powers, and its

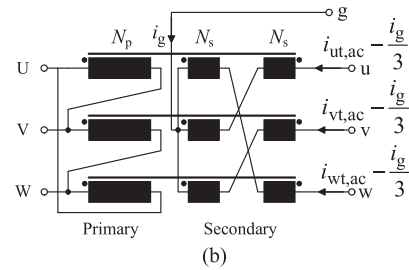
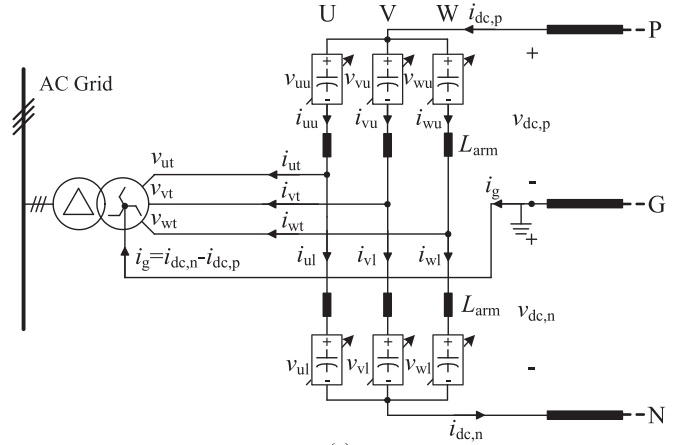


Fig. 4. Proposed configuration for bipolar MVDC distribution. (a) Schematic of the MMC with the zigzag transformer. (b) Schematic of the winding connection of the zigzag transformer.

maximum root-mean-square (RMS) value is as high as two-thirds of the rated dc-link current. Thus, the power rating of the auxiliary zigzag grounding transformer has to be around 60% of that of the grid interface transformer.

In this letter, an MMC with a zigzag transformer is proposed for bipolar MVDC distribution systems. By employing a delta-zigzag transformer for ac-grid connection with a dedicated operation scheme, an MMC can provide a full bipolar operation capability such that the positive and the negative poles on the dc side can be independently controlled. The significant advantage of the proposed scheme compared to the concepts in [7] and [9] is that, it requires no additional component and results in no penalty of increased current rating to the grid interface transformer. In addition, the voltage rating of the MMC can be increased simply by increasing the number of sub-modules (SMs) and the flexibility of the MMC can be exploited. Thus, the proposed scheme would be a promising solution for bipolar MVDC distribution systems.

II. DESCRIPTION OF THE PROPOSED CONFIGURATION

The schematic of the proposed configuration based on an MMC and a zigzag transformer is depicted in Fig. 4(a). The MMC is connected to an ac grid via the zigzag transformer. The neutral point of the bipolar dc distribution system is connected to the ground, and it is also connected to the star point of the zigzag transformer. The primary side of the transformer is delta connected in order to provide a circulating path for the third-order current caused by the core nonlinearity phenomena [8].

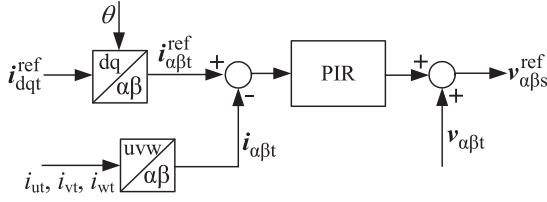


Fig. 5. Block diagram of the transformer current controller.

On the secondary side of the transformer, the turn numbers of two windings are identical and they are connected in such a way that the magnetic fluxes induced by the zero-sequence winding current are canceled out at each core. In case of the dc-pole power unbalance, a dc current i_G flows via the star point of the transformer secondary side into the ground. If the winding current is controlled such that the dc ground current i_G homogeneously distributes in three phases, then it does not result in core flux bias of the transformer [9]. Thus, the zigzag transformer can operate continuously without saturation even if a dc current flows via the star point. Since the dc magnetic flux is canceled out in the core, it would not result in the stray flux outside the core as in a three-limb inductor. It should be also noted that the zero-sequence impedance of the zigzag transformer is in the same range of the leakage inductance [9], and it enables a fast dynamic response of the zero-sequence current, which occurs in case of the dc-pole power unbalance.

When the star point is floated, an arm current of an arbitrary “x” phase of the MMC includes three components: the transformer current i_{xt} , the dc-link current i_{dc} , and the circulating current i_{xcir} , respectively, and each component can be controlled independently [10], [11]. When the star point is connected to the dc-side neutral point, an arm current would also include the component of the ground current. The transformer winding current includes two components, namely, the ac current, which is a positive-sequence component and the dc ground current, which is a zero-sequence component as (1). The upper and lower arm currents of “x” phase are presented by (2) and (3)

$$i_{xt} = i_{xt,ac} - \frac{i_g}{3} = i_{xt,ac} - \frac{i_{dc,n} - i_{dc,p}}{3} \quad (1)$$

$$i_{xu} = \frac{i_{xt,ac}}{2} - \frac{1}{2} \cdot \frac{i_g}{3} + \frac{1}{3} \cdot \frac{i_{dc,p} + i_{dc,n}}{2} + i_{xcir} \quad (2)$$

$$i_{xl} = -\frac{i_{xt,ac}}{2} + \frac{1}{2} \cdot \frac{i_g}{3} + \frac{1}{3} \cdot \frac{i_{dc,p} + i_{dc,n}}{2} + i_{xcir}. \quad (3)$$

The block diagram of the transformer current controller is depicted in Fig. 5, where the term v_{xs} is the voltage component synthesized by the MMC, which can regulate the transformer current independently [10]. The transformer current is regulated in the stationary reference frame by a proportional–integral–resonant (PIR) controller. The resonant controller enables the line-frequency ac component of the winding current tracking its reference, which is associated with the reactive and active power control, and the integral controller nullifies the dc differential component in the transformer current. Thus, it is guaranteed that the dc ground current flows homogeneously into three-phase

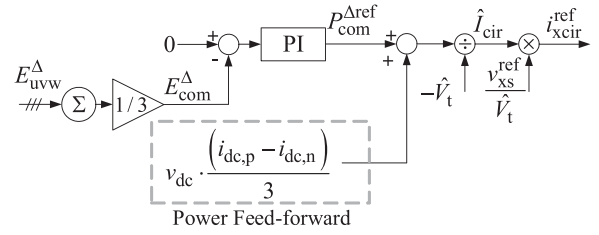


Fig. 6. Block diagram of the power unbalance feed-forward controller.

windings, and the transformer core saturation is consequently avoided.

In case of a power unbalance on the dc side, it results in SM-capacitor energy unbalance among upper arms and lower arms if no countermeasure is taken. The power disturbance introduced by the dc-side power unbalance can be compensated by injecting the positive-sequence ac component of the circulating current [10], [11]. To improve the dynamic performance of the SM-capacitor energy regulation, the unbalanced power between the positive and negative poles on the dc side should be utilized for the feed-forward control. The block diagram of the feed-forward controller is presented in Fig. 6. The power disturbance introduced by the dc-side power unbalance is calculated directly (depicted in the dashed block), thus the required magnitude of the positive-sequence circulating current can be calculated in a feed-forward manner for maintaining the SM-capacitor energy balance among upper and lower arms. The power errors caused by e.g., power conversion losses are compensated by the proportional–integral (PI) regulator in the arm-capacitor energy balancing controller [11] in the steady state.

In the steady state of the dc-side power unbalance, the positive-sequence circulating current continuously flows inside the MMC. The sum of the powers of two dc-side poles is handled by the transformer-side active power. In accordance with power balance in the steady state assuming no power conversion loss, the relationship can be described mathematically as (4), where \hat{V}_t and $\hat{I}_{t,ac}$ denote the magnitudes of transformer voltage and ac current, respectively. The difference of the powers of two dc-side poles is handled by the injected ac circulating current. In accordance with power balance [11] in the steady state assuming no power conversion loss, the relationship can be described mathematically as (5), where \hat{I}_{cir} denotes the magnitude of the injected circulating current

$$-\frac{3}{2} \cdot \hat{V}_t \cdot \hat{I}_{t,ac} = \frac{v_{dc}}{2} \cdot (i_{dc,p} + i_{dc,n}) \quad (4)$$

$$-\frac{3}{2} \cdot 2 \cdot \hat{V}_t \cdot \hat{I}_{cir} = \frac{v_{dc}}{2} \cdot (i_{dc,p} - i_{dc,n}). \quad (5)$$

III. ANALYSIS OF VOLTAGE AND CURRENT STRESS

Regarding the application of the proposed configuration for bipolar MVDC distribution, one of the main concerns is whether it results in penalty of increased voltage or current stress on the components. In this section, it is analyzed in a mathematical way to show that no extra stress would be imposed on the components.

A. Arm Current

Since the arm current directly flows through the power-semiconductor devices of SMs, its magnitude and RMS value would be a concern. Assuming that the MMC consumes or provides no reactive power and the voltage across the arm inductor is negligible compared to the transformer voltage, the arm currents of “x” phase can be represented as (6) and (7) by substituting (4) and (5) into (2) and (3)

$$\begin{aligned} i_{xu} &= i_{xt,ac} \cdot \frac{i_{dc,p}}{i_{dc,p} + i_{dc,n}} + \frac{i_{dc,p}}{3} \\ &= -\frac{v_{dc}}{3\hat{V}_t} \cdot i_{dc,p} \cdot \sin(\omega \cdot t) + \frac{i_{dc,p}}{3} \end{aligned} \quad (6)$$

$$\begin{aligned} i_{xl} &= -i_{xt,ac} \cdot \frac{i_{dc,n}}{i_{dc,p} + i_{dc,n}} + \frac{i_{dc,n}}{3} \\ &= \frac{v_{dc}}{3\hat{V}_t} \cdot i_{dc,n} \cdot \sin(\omega \cdot t) + \frac{i_{dc,n}}{3}. \end{aligned} \quad (7)$$

From (6) and (7), it can be concluded that the arm current is virtually linear with respect to the power of the corresponding pole, which means that two poles can operate independently. Thus, the MMC can operate in a bipolar manner without resulting in increased arm current stress.

B. SM-Capacitor Voltage

The SM-capacitor voltage may be another concern since it is directly imposed on the power-semiconductor devices. The dynamic of the SM-capacitor energy of the upper and lower arms can be modeled as (8) and (9), which lead to SM-capacitor voltage ripples. Since the arm output voltage v_{xu} and v_{xl} are almost identical over different operating points and the arm current is linear with respect to the corresponding dc-pole power, no increased voltage stress results from the dc-pole power unbalance

$$\frac{dE_{xu}}{dt} = v_{xu} i_{xu} \quad (8)$$

$$\frac{dE_{xl}}{dt} = v_{xl} i_{xl}. \quad (9)$$

C. Transformer Winding Current

Regarding the manufacturing of the transformer, the RMS value of the winding current is one of the key influencing factors on costs. The RMS value of the winding current can be calculated analytically by (10). The winding RMS current is contributed by one-third of the dc ground current and the ac active current. The dc ground current is proportional to the power difference between two poles, and the ac active current is proportional to the total power of two poles, as shown by (10). It is interesting to note that if the powers of dc poles are unbalanced, the dc ground current increases but the ac active current decreases compared to the balanced situation due to the reduced total dc-link power. From (10), it can be concluded mathematically that the maximum of the winding RMS current occurs when $i_{dc,p} = 1$ pu, $i_{dc,n} = 1$ pu or $i_{dc,p} = -1$ pu, $i_{dc,n} = -1$ pu, which corresponds to the full-power situations when dc-pole powers are balanced. It means

TABLE I
PARAMETERS OF THE SIMULATED SYSTEM

Transformer	
Transformer secondary-side voltage	10 kV
Transformer power rating	20 MVA
MMC converter	
Rated power	20 MW
Rated dc-link voltage	± 10 kV
Rated dc-link current	1 kA
Number of SMs per arm	20
Rated sub-module capacitor voltage	1.0 kV
Capacitance of sub-module capacitor	9 mF
Inductance of arm inductor	1 mH
Controller sampling frequency	10 kHz

that the current rating of the zigzag transformer just needs to be designed as large as that of the grid interface transformer which is used in the case of monopole dc link

$$\begin{aligned} I_{t,rms} &= \sqrt{\left(\frac{i_g}{3}\right)^2 + \left(\frac{\hat{I}_{t,ac}}{\sqrt{2}}\right)^2} \\ &= \sqrt{\left(\frac{i_{dc,p} - i_{dc,n}}{3}\right)^2 + \left(\frac{v_{dc}(i_{dc,p} + i_{dc,n})}{3 \cdot \sqrt{2} \cdot \hat{V}_t}\right)^2}. \end{aligned} \quad (10)$$

The manufacturing cost of the zigzag transformer would be higher than that of the normal wye- or delta-connected grid interface transformer with the same voltage and current ratings due to its more complicated winding connection. However, it can enable a full bipolar operation capability of a single MMC without increasing the transformer current rating and can significantly enhance the flexibility of dc grids. Moreover, it does not require an auxiliary electronic or magnetic device with a considerably high power rating, as the schemes in Figs. 1(c), 2, and 3.

In summary, a power unbalance of two poles on the dc side does not result in any extra voltage or current stress on the components. Thus, by connecting the transformer secondary side in a zigzag structure, as shown in Fig. 4(b), and employing the dedicated operation scheme, an MMC can establish a bipolar dc distribution system without any extra cost.

IV. SIMULATION AND EXPERIMENTAL RESULTS

A. Simulation Results

To verify the validity of the proposed configuration, a computer simulation has been performed based on PLECS. The simulation parameters are listed in Table I. Saturable core model is used in the simulation of the zigzag transformer.

In Fig. 7(a), simulation results are shown while the dc-pole power ($p_{dc,p}, p_{dc,n}$) changes from (1 pu, 1 pu) to (1 pu, 0 pu) when $t = 1.5$ s and changes from (1 pu, 0 pu) to (1 pu, -1 pu) when $t = 1.6$ s. In Fig. 7(b), simulation results are shown while the dc-pole power ($p_{dc,p}, p_{dc,n}$) changes from (-1 pu, -1 pu) to (-1 pu, 0 pu) when $t = 2.5$ s and changes from (-1 pu, 0 pu) to (-1 pu, 1 pu) when $t = 2.6$ s. In simulation results shown in

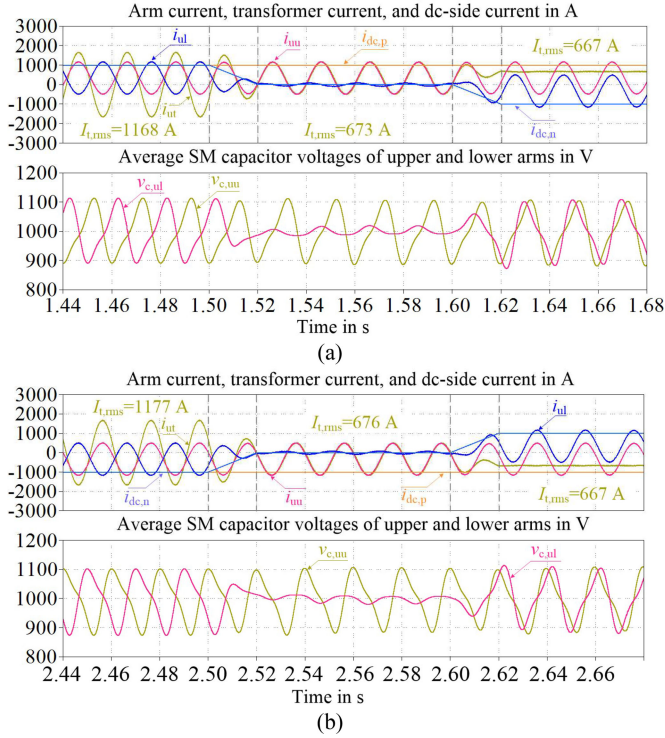


Fig. 7. Simulation results of the proposed configuration in different operation conditions. (a) Negative-pole power changes from 1 pu to -1 pu and the positive-pole power remains constant at 1 pu. (b) Negative-pole power changes from -1 pu to 1 pu and the positive-pole power remains constant at -1 pu.

both Fig. 7(a) and (b), the positive-pole power is kept constant while the negative-pole power varies. The upper arm current is kept constant, while the lower arm current varies linearly in accordance with the negative-pole power.

It is clearly shown in the simulation results that the arm current and the SM-capacitor voltage over the whole operation range does not exceed the values of the symmetric rated power operation. The maximum transformer RMS current occurs while two dc poles operate at the rated power in a symmetric manner. This verifies that by employing a 20-MVA zigzag transformer as a grid interface transformer, it is possible to operate a 20-MW MMC in a bipolar manner such that both dc poles can operate fully independently at a power rating of 10 MW. The MMC is well controlled, and the zigzag transformer does not saturate even if a dc current flows through the windings.

An identical MMC with a delta-*wye* transformer as a grid interface transformer and a zigzag transformer as a grounding device, as shown in Fig. 3, is simulated with the same scenarios for comparison. The dedicated operation method proposed in this letter is performed to the MMC, and the simulation results are shown in Fig. 8. The arm current and the SM-capacitor voltage of the MMC are identical to the case of the proposed configuration shown in Fig. 7. The maximum RMS current of the grid interface transformer occurs while two dc poles operate at the rated power in a symmetric manner, and the maximum RMS current of the auxiliary zigzag grounding transformer occurs while two dc poles operate at the rated power but with opposite direction. Thus, in order to enable a bipolar operation

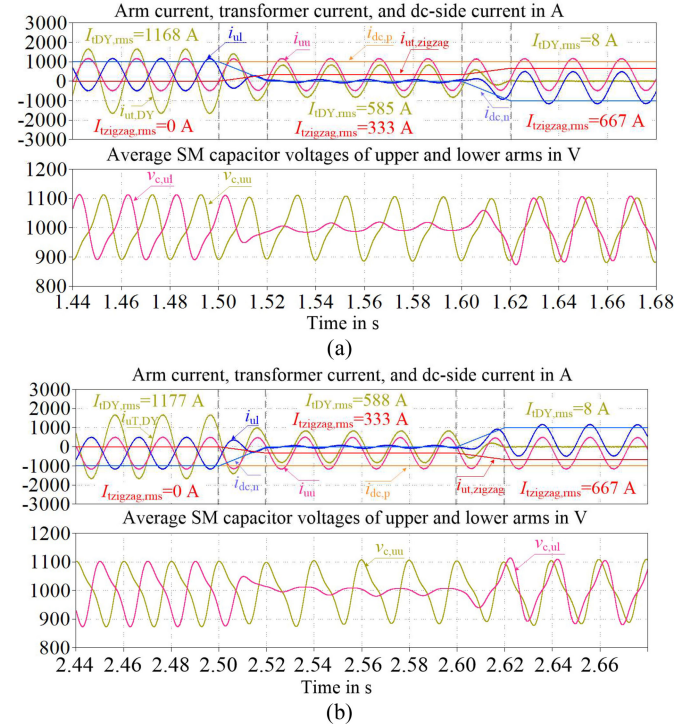


Fig. 8. Simulation results of the configuration with an auxiliary zigzag ground-ing transformer in different operation conditions. (a) Negative-pole power changes from 1 pu to -1 pu and the positive-pole power remains constant at 1 pu. (b) Negative-pole power changes from -1 pu to 1 pu and the positive-pole power remains constant at -1 pu.

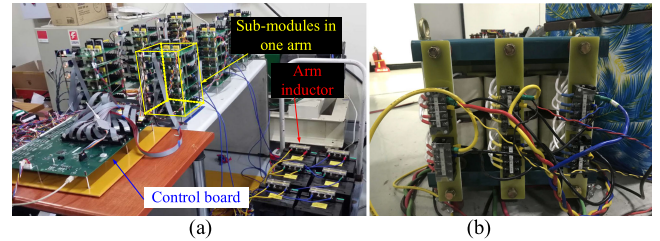


Fig. 9. Experimental setup. (a) MMC prototype. (b) Employed zigzag transformer.

capability, a 20-MW MMC requires a 20-MVA grid interface transformer and an 11.5-MVA zigzag grounding transformer additionally. On the contrary, the grid interface transformer and the zigzag grounding transformer are fully integrated to a single 20-MVA delta-*zigzag* grid interface transformer in the proposed configuration.

B. Experimental Results

A scaled-down laboratory MMC prototype shown in Fig. 9(a) with a zigzag transformer shown in Fig. 9(b) has been built up and tested. The circuit parameters are listed in Table II.

Experimental results when the dc-pole power is (1 pu, 1 pu), (1 pu, 0 pu), (1 pu, -1 pu), and (-1 pu, 1 pu) are shown in Fig. 10(a)–(d), respectively. Coinciding with the simulation results, the arm current and the SM-capacitor voltage do not exceed the limits at the symmetric rated power. The maximum transformer RMS current occurs when two dc poles operate at

TABLE II
PARAMETERS OF THE EXPERIMENTAL SETUP

MMC converter	
Transformer secondary-side voltage	135 V
Rated dc-link voltage	± 150 V
Rated dc-link current	10 A
Number of SMs per arm	6
Rated sub-module capacitor voltage	50 V
Capacitance of sub-module capacitor	5.4 mF
Inductance of arm inductor	4 mH
Controller sampling frequency	10 kHz

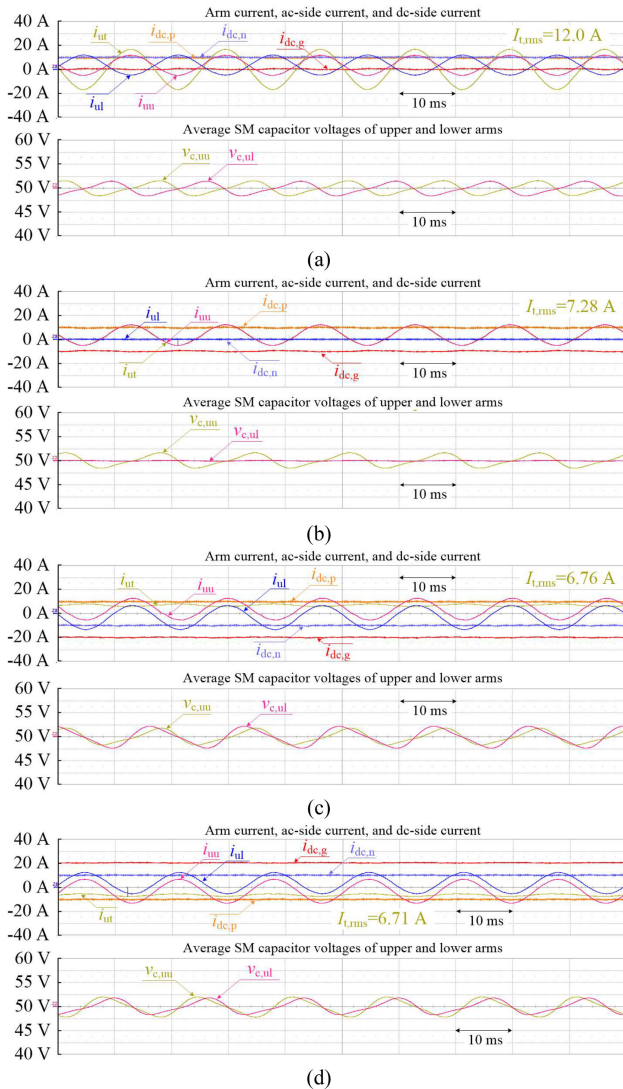


Fig. 10. Experimental results in different operating conditions of dc-pole power. (a) (1 pu, 1 pu). (b) (1 pu, 0 pu). (c) (1 pu, -1 pu). (d) (-1 pu, 1 pu).

the rated power symmetrically. Due to the zero-sequence flux cancellation, the transformer is not saturated even if a significant dc current flows in the windings.

It is interesting to note that the ac component of the transformer current is almost zero when the dc-pole power is (1 pu, -1 pu) or (-1 pu, 1 pu) in both simulation and experiment results, and the transformer current includes a dc component,

which results from the ground current due to asymmetric dc-pole powers. It means that the active power of the transformer is zero, and a power circulates between the positive and the negative poles of the MMC. One might argue that it results in extra losses. However, it should be noted that, in a bipolar distribution system, a circulating power is inevitable in case of a dc-pole power unbalance even if the distribution system is established based on the power balancer shown in Fig. 1(c) or two independent ac-dc converters, as shown in Fig. 1(b). Thus, the circulating power is not the problem of the proposed configuration, but it comes from the nature of an unbalanced dc power itself.

V. CONCLUSION

In this letter, a bipolar dc distribution system based on MMC with a zigzag transformer has been proposed. By connecting a zigzag transformer as a grid interface transformer with the dedicated operation method, the MMC can operate in a fully bipolar manner without penalty of increased voltage or current stress on components even under severely unbalanced dc power in positive and negative poles. The power rating of the proposed system, including the transformer, is identical to the conventional MMC-based monopole distribution system. Validity of the proposed concept has been verified by both simulations and experiments.

REFERENCES

- [1] R. W. De Doncker, "Power electronic technologies for flexible dc distribution grids," in *Proc. IEEE Int. Power Electron. Conf.*, Hiroshima, Japan, 2014, pp. 736–743.
- [2] P. Salonen, T. Kaipia, P. Nuutinen, P. Peltoniemi, and J. Partanen, "An LVDC distribution system concept," in *Proc. Nordic Workshop Power Ind. Electron.*, 2008, pp. A3-1–A3-16.
- [3] S. Rivera, B. Wu, S. Kouro, V. Yaramasu, and J. Wang, "Electric vehicle charging station using a neutral point clamped converter with bipolar dc bus," *IEEE Trans. Ind. Electron.*, vol. 62, no. 4, pp. 1999–2009, Apr. 2015.
- [4] H. Kakigano, Y. Miura, and T. Ise, "Low-voltage bipolar-type dc microgrid for super high quality distribution," *IEEE Trans. Power Electron.*, vol. 25, no. 12, pp. 3066–3075, Dec. 2010.
- [5] J. Lago, J. Moia, and M. L. Heldwein, "Evaluation of power converters to implement bipolar dc active distribution networks—DC-DC converters," in *Proc. IEEE Energy Conversion Congr. Expo.*, 2011, pp. 985–990.
- [6] Y. Gu, W. Li, and X. He, "Analysis and control of bipolar LVDC grid with dc symmetrical component method," *IEEE Trans. Power Syst.*, vol. 31, no. 1, pp. 685–694, Jan. 2016.
- [7] Y. Li, A. Junyent-Ferré, and J. Rodriguez-Bernuz, "A three-phase active rectifier topology for bipolar dc distribution," *IEEE Trans. Power Electron.*, vol. 33, no. 2, pp. 1063–1074, Feb. 2018.
- [8] J. H. Harlow, *Electric Power Transformer Engineering*. Boca Raton, FL, USA: CRC Press, 2012.
- [9] H. Wang, G. Tang, Z. He, and J. Yang, "Efficient grounding for modular multilevel HVDC converters (MMC) on the ac side," *IEEE Trans. Power Del.*, vol. 29, no. 3, pp. 1262–1272, Jun. 2014.
- [10] S. Cui, S. Kim, J. J. Jung, and S. K. Sul, "A comprehensive cell capacitor energy control strategy of a modular multilevel converter (MMC) without a stiff dc bus voltage source," in *Proc. IEEE Appl. Power Electron. Conf. Expo.*, 2014, pp. 602–609.
- [11] S. Cui and S. K. Sul, "A comprehensive dc short-circuit fault ride through strategy of hybrid modular multilevel converters (MMCs) for overhead line transmission," *IEEE Trans. Power Electron.*, vol. 31, no. 11, pp. 7780–7796, Nov. 2016.
- [12] Y. Park, S. K. Sul, C. H. Lim, W. C. Kim, and S. H. Lee, "Asymmetric control of dc-link voltages for separate MPPTs in three-level inverters," *IEEE Trans. Power Electron.*, vol. 28, no. 6, pp. 2760–2769, Jun. 2013.
- [13] C. Wang and Y. Li, "Analysis and calculation of zero-sequence voltage considering neutral-point potential balancing in three-level NPC converters," *IEEE Trans. Ind. Electron.*, vol. 57, no. 7, pp. 2262–2271, Jul. 2010.